Energy & Environmental Science

ROYAL SOCIETY OF CHEMISTRY

COMMUNICATION

View Article Online
View Journal | View Issue

Check for updates

Cite this: *Energy Environ. Sci.*, 2021, **14**, 4410

Received 2nd March 2021,
Accepted 7th June 2021

DOI: 10.1039/d1ee00650a

rsc.li/ees

Open Access Article. Published on 01 Julie 2021. Downloaded on 2026-05-13 5:16:18 vm..
This article is licensed under a Creative Commons Attribution 3.0 Unported Licence.

Efficiency gains for thermally coupled solar hydrogen production in extreme cold†

Moritz Kölbach, [ab] Kira Rehfeld [c] and Matthias M. May *[b]

Hydrogen produced from water using solar energy constitutes a sustainable alternative to fossil fuels, but solar hydrogen is not yet economically competitive. A major question is whether the approach of coupling photovoltaics *via* the electricity grid to electrolysis is preferential to higher levels of device integration in 'artificial leaf' designs. Here, we scrutinise the effects of thermally coupled solar water splitting on device efficiencies and catalyst footprint for sub-freezing ambient temperatures of −20 °C. These conditions are found for a significant fraction of the year in many world regions. Using a combination of electrochemical experiments and modelling, we demonstrate that thermal coupling broadens the operating window and significantly reduces the required catalyst loading when compared to electrolysis decoupled from photovoltaics. Efficiency benefits differ qualitatively for dual- and triple-junction solar absorbers, which has implications for the general design of outdoor-located photoelectochemical devices. Similar to high-efficiency photovoltaics that reached technological maturity in space, application cases in polar or alpine climates could support the scale-up of solar hydrogen at the global scale.

Broader context

The fossil fuel supply of remote high-latitude and high-altitude regions with cold climates, such as research stations in Antarctica, causes challenges including expensive logistics associated with the transport, potential contamination by spillage events, and further contributions to anthropogenic carbon dioxide emissions. In contrast, locally produced hydrogen is a greenhouse gas-free and environmentally benign energy carrier that can be easily stored in gas bottles at very low temperatures. Here, we discuss the potential of a decentralised, small-scale hydrogen production under sub-freezing ambient temperatures. To achieve a high level of autonomy of small-scale solar hydrogen production, and to compensate possible efficiency losses due to low outdoor temperatures, we investigate a thermally coupled and membrane-free device design. We quantify the efficiency benefits of thermal coupling and demonstrate the first solar water-splitting device operating at −20 °C. Besides niche applications in remote world regions, our work is also relevant for the design of highly efficient thermally coupled solar water splitting based on III–V/Si or Perovskite/Si tandem cells, be it in a wired design or with the absorber fully immersed in the electrolyte.

Fossil fuels constitute a versatile and large fraction of our energy sources, but contribute significantly to anthropogenic warming.[1] Solar-driven water splitting (aka electrolysis) produces hydrogen, an alternative energy carrier free of greenhouse gases, sustainably and without the limitations of wind power and biomass.[2–4] The main obstacle preventing large-scale implementation are currently the comparatively high production costs. However, logistics for fossil fuels can also be expensive and environmentally hazardous, in particular for the year-round energy supply of remote research bases such as the Neumayer Station in Antarctica or Paranal observatory in Chile. Therefore, local hydrogen production can become both economically and environmentally favourable, but is challenging in the often cold environments.[5,6]

The currently most mature approach for solar-driven hydrogen production is to supply polymer electrolyte membrane electrolysers with electricity from photovoltaic (PV) solar cells *via* the grid.[2,7–9] The complete separation of light absorption and electrolysis does, however, come with electrical and thermal losses. Firstly, an additional DC-to-DC converter is required.[7] Secondly, internal thermalisation, *i.e.* de-excitation of charge-carriers to the band edges under the release of phonons, reduces the extractable energy of excited electron–hole pairs. In addition, transmission losses of low-energy photons with energies below the bandgap of the light-absorbing semiconductor limit the current.[3,10] The heat generated by these two latter loss mechanisms has the potential to benefit catalysis. Therefore, a thermally tightly coupled water-splitting device – with

[a] *Helmholtz-Zentrum Berlin für Materialien und Energie GmbH, Institute for Solar Fuels, Hahn-Meitner-Platz 1, 14109 Berlin, Germany*
[b] *Universität Ulm, Institute of Theoretical Chemistry, Lise-Meitner-Str. 16, 89069 Ulm, Germany. E-mail: matthias.may@uni-ulm.de*
[c] *Ruprecht-Karls-Universität Heidelberg, Institute of Environmental Physics, INF 229, 69120 Heidelberg, Germany*

† Electronic supplementary information (ESI) available: Full Experimental section, input parameters for calculations and additional data. See DOI: 10.1039/d1ee00650a

This journal is © The Royal Society of Chemistry 2021

Open Access Article. Published on 01 Julie 2021. Downloaded on 2026-05-13 5:16:18 vm..
This article is licensed under a Creative Commons Attribution 3.0 Unported Licence.

the light absorber immersed into the electrolyte or not – represents a highly attractive concept. Such a design uses the waste heat of the absorbers to decrease the internal device electrical resistance and reduce the requirements for the catalysts, while simultaneously cooling the absorbers and hence boosting their efficiency.[7,11] Furthermore, a design that allows safe product separation without a degradation- and failure-prone membrane also reduces costs and increases operating life.[12] Recently, the beneficial effects of thermally coupled water splitting at ambient temperatures were demonstrated.[13] Solar water-splitting research in general has just recently started to consider the influence of colder ambient temperatures on device operation in the temperate zones.[14] So far, however, the impact of very low temperatures over extended times as found in high-latitudes, high-altitudes or winters in the temperate zones on operation have not been considered.

In this work, we investigate a route of expanding the thermal window that makes solar water splitting feasible down to an outdoor temperature of −20 °C. Climate data analysis shows that many world regions at high latitudes or altitudes could benefit from our considerations, prominent examples are Antarctica or the Himalaya region. We use a numerical device model to explore the influence of such low temperatures on the solar-to-hydrogen (STH) efficiency of solar water splitting devices and quantify the beneficial effects of thermal coupling and a suitable device insulation. These predictions are scrutinised under idealised laboratory conditions and the first solar water splitting device operating at −20 °C is demonstrated. We can also show that these benefits differ qualitatively for dual- and triple-junction solar absorbers, which has significant implications for the general design of outdoor-located photoelectrochemical devices. Finally, we discuss the energy supply of high-latitude and high-altitude remote research stations as a first potentially economic competitive implementation of our considerations.

Current large-scale technologies for water splitting operate at temperatures between 50 and 1000 °C.[9] Meanwhile, laboratory studies for solar water splitting typically employ ambient temperatures of about 20 °C. For small- to medium-scale, distributed hydrogen production, however, the impact of outdoor temperatures on device operation must be considered. While the volumetric density of dissipated heat of electrolysers in the MW-range are often large enough to require cooling, this changes for smaller plants that are more effectively cooled by outdoor temperatures. In the limit of small-scale applications, such as the powering of weather stations, process temperatures will, without external heating, very closely follow ambient conditions.

Yet the mean annual temperatures of a considerable part of the world is below the freezing point of water (Fig. 1a). Low electrolyte temperatures lead to losses from higher catalysis and ion transport overpotentials, but also cause issues for (near-)neutral electrolytes, frequently used for solar water splitting,[17] that do not depress the freezing point of water sufficiently. Hydrogen production would then cease and the volumetric expansion of freezing water can damage the reactor. The energy harvesting potential for conventional solar hydrogen production can be evaluated from Fig. 1c, in which we show the

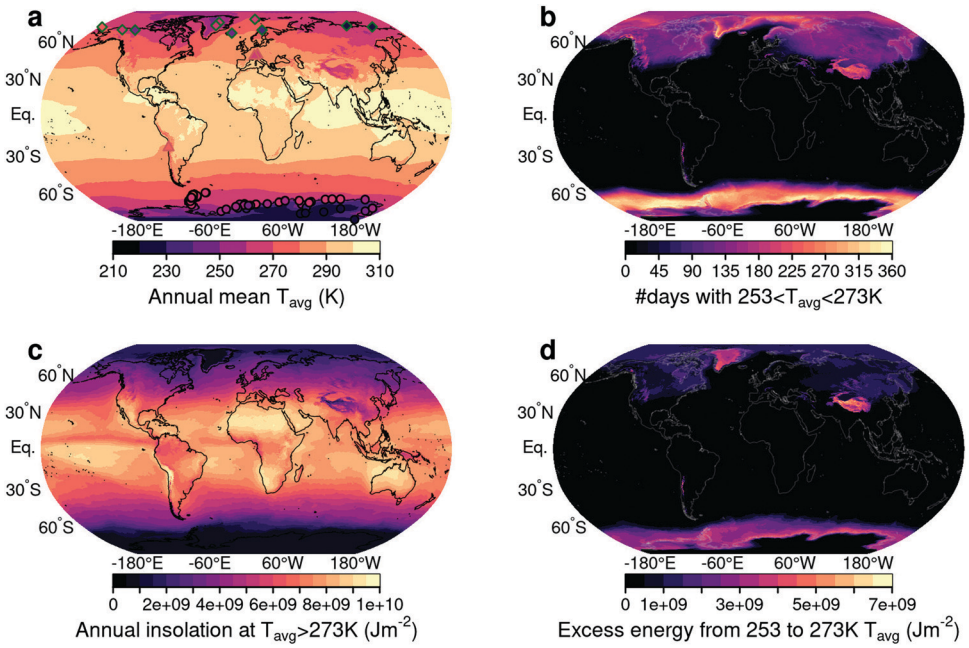

Fig. 1 Global benefit of thermally coupled solar water splitting in a temperature envelope between −20 °C and 0 °C. (a) Global distribution of annual mean temperature. Symbols show locations of high-latitude and high-altitude research stations. (b) Number of days in the cold temperature envelope considered for the thermally integrated device. (c) Solar radiation that can be harvested at daily mean temperatures above 273 K. (d) Global distribution of excess energy that can be harvested in the daily-mean temperature envelope between 253 and 273 K. All results derived here are based on reanalysis data[15,16] for the year 2019.

Open Access Article. Published on 01 Julie 2021. Downloaded on 2026-05-13 5:16:18 vm..
This article is licensed under a Creative Commons Attribution 3.0 Unported Licence.

annual cumulative available solar energy for days with mean temperatures above the freezing point of water. In colder regions, however, temperatures remain in a temperature envelope between −20 °C and 0 °C for a considerable fraction of the year (Fig. 1b). This would create the need for energy-intensive temperature stabilisation of the device. A distributed energy system that can operate with a maximum degree of autonomy would, however, be even more important in these regions, since they are typically more sparsely populated and fuel supply is associated with great expense and effort. Since the long-term storage of hydrogen in gas bottles at very low temperatures is not a challenge, it is a predestined energy carrier for these extreme climate conditions. Extending the ambient operating conditions for efficient, small-scale solar water splitting to the above-defined temperature envelope is feasible through the use of electrolytes with a low-freezing point (*e.g.* 30 wt% H_2SO_4). Efficiency losses due to the low operating temperatures can be compensated by tight thermal coupling and device insulation as discussed below in detail. Here, insulation refers to the reduced heat transfer between device and its surroundings, while thermal coupling enables heat transfer between absorber and electrolyte. Such a heat management would facilitate additional energy harvesting by solar hydrogen production in some regions considerably as depicted in Fig. 1d. Based on our considerations, solar hydrogen production could benefit in parts of China, Mongolia, the Himalayas, Russia, the Alpine region, Greenland, the Andean mountains, USA, Canada, and Antarctica. More than half of the world population is currently living in areas, where temperatures are in this envelope for at least 30 days per year.

The influence of low temperatures on the solar-to-hydrogen conversion efficiency of a solar water splitting device, as sketched in Fig. 2a, is characterised by two contrary effects. Firstly, there is the lower catalytic performance and higher ohmic losses of the electrochemical component, and secondly, the increased solar-cell efficiency, as indicated in Fig. 2b. Which one prevails depends on a number of device parameters, such as the ohmic cell resistance and the temperature coefficient of the solar-cell open-circuit voltage (V_{OC}). To understand these effects in detail and explore thermal coupling to compensate possible efficiency losses, we developed an open-source Python-based model combining solar-cell parameters, electrochemistry, and thermal fluxes. In short, the model predicts the STH efficiency based on the temperature-dependent current–voltage (*IV*) characteristics of the solar cell and catalysts by computing the operating temperature in an iterative, self-consistent cycle for a quasi-steady-state condition. This means that the absorbed luminous power equals the sum of the power used to split water at thermoneutral conditions plus the power dissipated by radiation and convection (see Fig. 2a).

The following calculations are based on a device consisting of high-efficiency dual- or triple-junction III–V solar cells together with Pt- and IrO_x-catalysts for hydrogen/oxygen evolution reaction (HER/OER), respectively. 30 wt% H_2SO_4 with a freezing point of −35 °C[19] was used in the model as the electrolyte. Consequently, the electrolyte stays liquid for all our experiments, further increase of the H_2SO_4-concentration could become necessary for freezing point suppression also during polar nights.[19] Note that one important parameter determining the device temperature is the area ratio $A_{housing}/A_{solar\text{-}cell}$,

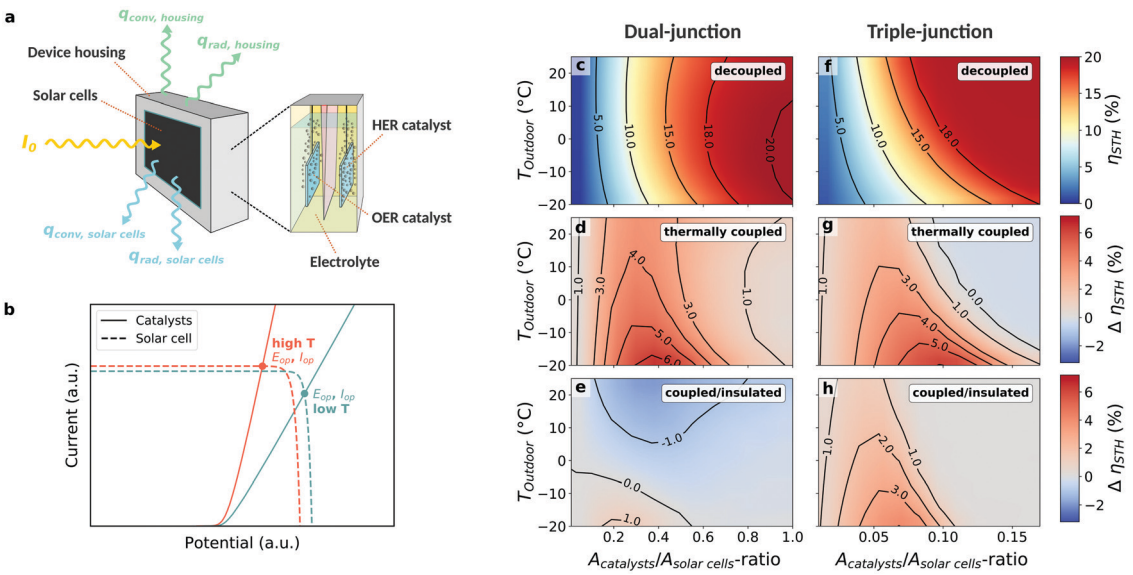

Fig. 2 Modelling the thermally integrated solar water splitting device. (a) Sketch of the thermally coupled device with the solar cell attached to the electrochemical compartment. A wedge separates gases forming at the catalyst-decorated electrodes. Radiative and convective heat flux into and out of the device are schematically indicated. (b) Qualitative influence of low temperatures on the solar cell and catalyst IV characteristics. (c–h) STH efficiencies and efficiency gains modelled by YaSoFo[18] as a function of the $A_{catalyst}/A_{solar\ cells}$-ratio, for the decoupled, thermally coupled, and coupled as well as insulated case using a dual-junction (c–e) and a triple-junction (f–h) solar cell. (d and g) Increase in absolute STH efficiency caused by thermal coupling in comparison to the non-coupled device. (e and h) Efficiency gain from insulation of the electrochemical compartment referring to the coupled configuration. For equilibrium temperatures, see ESI,† Fig. S2.

 This journal is © The Royal Society of Chemistry 2021

Open Access Article. Published on 01 Julie 2021. Downloaded on 2026-05-13 5:16:18 vm..
This article is licensed under a Creative Commons Attribution 3.0 Unported Licence.

influencing the heat dissipation from the housing by radiation and convection (see ESI,† Fig. S1). This ratio was fixed to a practical value of 2.5 in the following considerations, representing the case of small- to medium-scale applications. A description of the full model[18] and a list of all input parameters can be found in the ESI.† Note that a low-cost, but less-efficient alkaline device design could in principle also be realised using Si solar cells, $NiFeO_x$ (OER catalyst), NiMo (HER catalyst), and 18 wt% NaOH as an electrolyte. Similar to III–V solar cells for space applications,[10] costs of the absorber are, however, probably not a major issue for niche-applications in remote world regions, where the approach competes with the supply of conventional fuels that is associated with great expense and effort. As soon as the technology is established, costs can benefit from scale-up as well as from emerging low-cost, high-efficiency approaches[20,21] that would extend the commercial use case beyond just niche also into regions with better infrastructure. Such a development path from the niche to larger markets has already occurred for high-efficiency photovoltaics, which reached maturity in space applications.[10] The same considerations for scale-up apply to the catalysts. For initial applications, the $A_{catalyst}/A_{solar\text{-}cells}$-ratio could be adjusted to ensure operating potential below the maximum power point (MPP) for a high-efficiency triple-junction solar cell. However, for the long-term goal of producing hydrogen on a terawatt (TW) scale costs – but even more so materials availability – will play an important role. There, the use of low-performance, abundant catalysts (or low noble-catalyst loadings) is highly preferable and any additional voltage losses should be avoided as discussed below in detail. Therefore, the parameter ranges of $A_{catalyst}/A_{solar\text{-}cells}$ in the model were chosen to cover operating potentials close to the MPP.

Fig. 2c and f show the outdoor temperature-dependent STH efficiencies as a function of the $A_{catalyst}/A_{solar\text{-}cells}$-ratio for a thermally decoupled device based on a dual-junction (V_{OC} = 1.88 V) and triple-junction (V_{OC} = 2.7 V) solar cell, respectively. For the dual-junction, the STH efficiency initially increases, but then decreases with decreasing outdoor temperature implying that the device only benefits from improved solar-cell performance for moderate temperature decreases. Consequently, considering only a narrow temperature window[22,23] could lead to the unsubstantiated generalisation of a steadily increasing or decreasing efficiency with dropping temperature. Note that this effect is very sensitive to the V_{OC}, its temperature coefficient, and the ohmic resistance of the cell. A more negative V_{OC} temperature coefficient and a lower V_{OC}, for example, result in less or almost no decrease of the efficiency at very low temperature, while a higher ohmic cell resistance increases this effect (and *vice versa*, see ESI,† Fig. S3 and S4). The modelling of the triple-junction reveals a constant STH efficiency decrease with decreasing outdoor temperature, an effect that is more stable with respect to parameter variation. In this case, the lower performance of the electrochemical compartment always prevails. This can explained mainly by the higher ohmic potential loss caused by the higher catalyst current densities in the triple-junction device when working near the MPP (see ESI,† Fig. S5). Furthermore, large differences in temperature-coefficients of V_{OC} can also play a role, depending on material properties.

The absolute efficiency gain for a thermally coupled device design is illustrated in Fig. 2d and g. As expected, thermal coupling increases the absolute STH efficiency by up to 6% at low outdoor temperatures for configurations where the operating current of the device would otherwise drop below the MPP. To further increase the efficiency, we explored the influence of thermally insulating the device housing. In the model, aluminium foil was employed to reduce radiation losses and polystyrene was used to minimise further heat dissipation. The results are shown in Fig. 2e and h as an absolute efficiency change referring to the thermally coupled design. For the dual-junction, the insulation has a detrimental effect on parameter regions in which the efficiency increases with decreasing outdoor temperature, while it has a positive effect in regions where the efficiency decreases with decreasing outdoor temperature (also see ESI,† Fig. S4). For the triple-junction, where the efficiency steadily decreases with decreasing outdoor temperature, the insulation is always beneficial.

Fig. S3 (ESI†) shows, in a similar manner as Fig. 2c–h, the functional dependence with respect to the geometry-corrected distance, which is a measure for the electrode spacing, taking into account the device geometry. Again, we observe a qualitative difference for dual- and triple-junctions. This emphasises that these parameters span a multi-dimensional space and therefore must be carefully considered when designing a dual-junction device intended to operate at low temperatures. Only considering a subset in the parameter space is probably the reason for apparently contradictory observations in the literature.[14,22]

The insulation design of the electrochemical compartments could be further improved with the ongoing development of macroscopic thermal rectifiers that allow heat to transfer preferentially in one direction.[24] Such a rectifier would offer the possibility of creating and maintaining a thermal gradient between the electrochemical compartment and the solar cells, which could increase the efficiency boost for the device. The effective thermal gradient from the rectifier would depend on the variability of outdoor conditions (weather), as it does not transfer heat from cold to hot under steady-state conditions. Consequently, the quantitative benefit would depend on the location. Apart from conventional absorber materials like Si or III–V semiconductors, transition metal oxides are also feasible absorbers for photoelectrochemical water splitting.[11] Charge carriers in many of these oxides form small polarons resulting in a small drift mobility[25] implying that the carrier transport might be enhanced *via* thermal-activating.[26] This suggests that insulating an oxide-based device might not only increase the catalytic performance and lower the ohmic losses, but would be also beneficial for the photoabsorber.

To scrutinise our predictions under idealised laboratory conditions, we built a water-splitting device based on commercial triple-junction GaInP/GaInAs/Ge solar cells and commercial Pt- and IrO_x-catalysts. The electrodes were separated *via* a

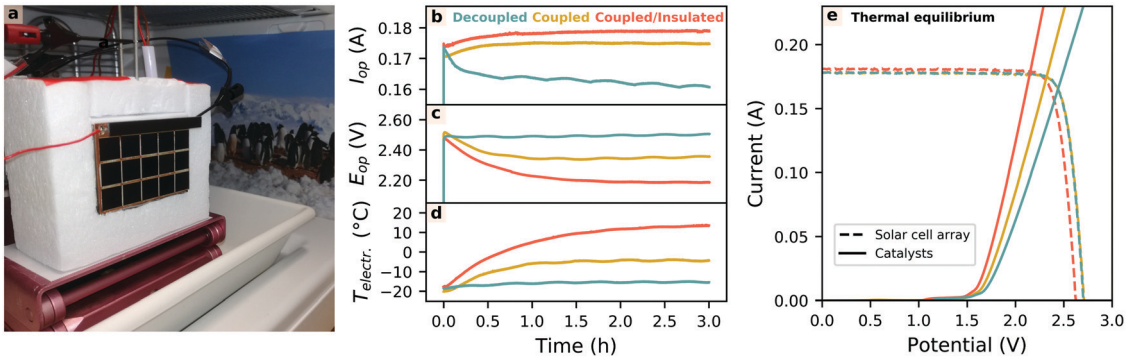

Fig. 3 Experimental validation of the thermally integrated solar-water-splitting device. (a) Device in the coupled/insulated configuration inside the cooling device. (b–d) Operating current, operating voltage, and electrolyte temperature of the decoupled, coupled, and coupled/insulated device configurations under simulated AM 1.5G illumination at −20 °C without an external bias. The illumination was turned on at t = 0. (e), IV curves of the solar-cell array and the Pt- and IrO_x-catalysts in a 2-electrode configuration of the respective configurations in thermal equilibrium, *i.e.* after the 3 h-measurements.

wedge for buoyancy-driven product separation as can be seen in ESI,† Fig. S6. Note that this membrane-less concept is a relatively novel approach and there are ongoing efforts to investigate the product crossover as a function of the cell geometry.[12] The $A_{catalyst}/A_{solar\text{-}cells}$-ratio was set to 0.34 and the total device resistance (including the multimeter) was 2.2 Ω at 21 °C. A freezer was modified with a window for illumination to simulate working conditions under cold climates (see Methods). This setup resulted in mean temperatures between −19.2 °C and −20.5 °C during the illumination (see ESI,† Fig. S7). Fig. 3b–d show the operating current (I_{op}), the operating voltage (E_{op}), and the electrolyte temperature (30 wt% H_2SO_4) of the device under AM 1.5 illumination for 3 h for three configurations: (i) thermally decoupled, (ii) thermally coupled, and (iii) thermally coupled with an insulation as shown in Fig. 3a (see Methods section in the ESI†). The IV curves of the solar-cell array and the catalysts in a 2-electrode measurement of the respective configurations, recorded directly after the 3 h measurement, are shown in Fig. 3e. For the decoupled configuration, I_{op} decreases from an initial value of 0.173 A to a value of 0.161 A, whereas for the coupled and coupled/insulated configuration, I_{op} continuously increases up to a value of 0.175 A and 0.179 A, respectively. This translates into conservatively estimated STH efficiencies of 10.3% (uncoupled), 11.2% (coupled), and 11.4% (coupled/insulated) on the module scale using the Gibb's Free Energy of 2 × 1.23 eV per hydrogen molecule for the STH definition (see Methods). The electrolyte temperature in the decoupled configuration only slightly increases due to operation beyond the thermoneutral voltage, while the solar cells heat up, lowering their open-circuit potential. Hence, the operating potential slightly increases and moves beyond the MPP of the solar-cell array, causing the sharp decrease in the operating current. For the coupled and coupled/insulated configuration, the effect of the beneficial increase of the electrolyte temperature reaching −4.5 °C and 13.5 °C, respectively, after 3 h (Fig. 3d) prevails over the solar-cell efficiency loss as predicted in our model, resulting in the increase of the operating current and a decrease of the operating potential. For the insulated configuration, it can be clearly seen in Fig. 3e that the additional increase of the catalyst performance (ΔV = 0.18 V at 0.179 A) in comparison to the coupled configuration is not offset by the additional loss of V_{OC} (ΔV_{OC} = 0.08 V) caused by the higher device temperature.

The energy supply for research stations in high-latitude regions such as Antarctica represents an ideal test application for our considerations. There are ongoing efforts to shift the power supply away from the use of fossil fuels towards renewable energy systems,[27,28] also for reasons of contamination due to spillage events. Here, hydrogen was indeed already proposed as a future energy carrier,[5] and initial practical experience with an indoor, wind-powered electrolyser was gained.[6] While the overall impressions and results were positive, the complexity of the system caused some technical issues and hence relatively high maintenance efforts.[6] Here, a device that operates outdoors with a maximum degree of autonomy could be highly advantageous and represent the first economically competitive case for thermally coupled solar water splitting. Moderate light concentration could, in principle, reduce the costs for hydrogen production. However, this depends on the location. In near-polar regions, diffuse irradiation that cannot be concentrated can prevail the direct radiation in the solar spectrum,[29] which would consequently even reduce the device efficiency when using light concentration. Higher current densities will, on the other hand, emphasise efficiency losses from ion transport and therefore the beneficial effects of thermal coupling (see ESI,† Fig. S8, S9, and the Supplementary note 1 for an assessment with the concentration factor of 1.5 and 2).

Beyond Antarctica, many research stations across the globe are situated in other remote locations at high-latitude and/or high-altitude (Fig. 1a). In almost all of the 100 stations, we considered, the mean annual temperature, $T_{avg,y}$, remains below the freezing point of water for large parts of the year (Fig. 4). The developments we report here will allow to expand the thermal window that makes solar hydrogen production feasible for most stations, except for in the Antarctic interior.

Open Access Article. Published on 01 Julie 2021. Downloaded on 2026-05-13 5:16:18 vm..
This article is licensed under a Creative Commons Attribution 3.0 Unported Licence.

 This journal is © The Royal Society of Chemistry 2021

Open Access Article. Published on 01 Julie 2021. Downloaded on 2026-05-13 5:16:18 vm..
This article is licensed under a Creative Commons Attribution 3.0 Unported Licence.

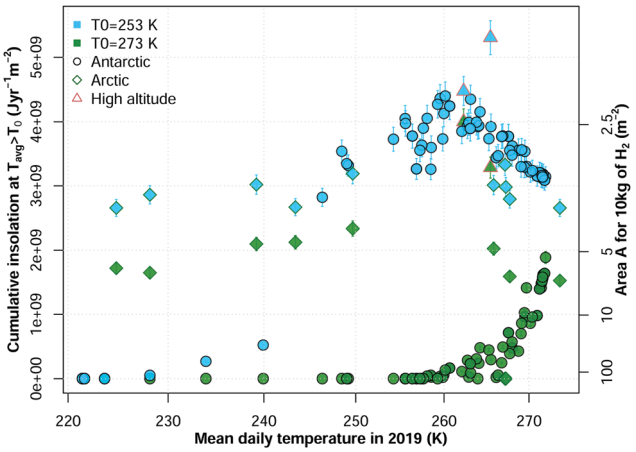

Fig. 4 Solar hydrogen production benefit at research stations. Scatterplot of mean site temperature against the cumulative insolation for days above the temperature threshold T_0 (left y-axis) and the effective module area for an annual production of 10 kg H_2 at 12% STH efficiency (right y-axis). Error bars denote the estimated 10% relative error (Methods). Symbols denote the location of the field sites and research stations as Antarctic (below 60°S, black circles), Arctic (above 60°N, green diamonds) and high-altitude non-polar stations (red triangles), see ESI,† Table S5 and ref. 31. With the expansion of the thermal window down to a threshold temperature of T_0 = 253 K (blue shading), efficient, distributed solar water splitting is feasible for most research stations with low module areas. In contrast, for a threshold temperature of T_0 = 273 K, (green shading) only some high-altitude and Arctic sites could benefit.

A realistic hydrogen fuel-cell efficiency is 65% (lower heating value).[30] Then, powering a Raspberry Pi computing device (P_{RPi} = 4 W) for an autonomous measurement device year-round at the Neumayer III station (70.68°S, 8.27°W, $T_{avg,y}$ = −15.5 °C) would prospectively require a module area of 0.41 m^2, whereas at Paranal observatory (Chile, 24.63°S, 70.40°W, $T_{avg,y}$ = 0.4 °C) 0.18 m^2 would suffice.

Hydrogen storage itself does, however, introduce an energy overhead mainly required for the compression, be it mechanical by an external compressor or directly in the electrochemical cell. Especially for stationary applications, highest energy densities might not be required and storage at 50 bar could be sufficient. Assuming an ideal gas and −20 °C, compression to this pressure would require ∼2.1 kW h per kg of produced hydrogen, and without making use of the stored mechanical energy upon release of the gas, the area values displayed in Fig. 4 would increase by ∼11% using the same fuel cell efficiency for the compressor as for the consumer device. Operating the production device itself can in principle be achieved without overhead, especially if the electrolyte is chosen to stay liquid even at the lowest expected temperature. An overhead can arise at the consumer end, where the fuel cell might require additional heating to stay within its operation temperature window. This heating could be achieved by ramping up the power of the fuel cell or, alternatively, by catalytic combustion.[32] This will strongly depend on design aspects, such as insulation, of the consumer device.

For the long-term goal of producing hydrogen on a TW scale, where materials abundance for both light absorber and catalysts will play an important role as discussed above, the increase of performance by thermal coupling and insulation offers benefits in three major areas: firstly, it can increase the solar-to-hydrogen efficiency by shifting the operating point of a given device to higher current densities or using solar cells with lower bandgaps.[13] Furthermore, the amount of catalyst loading can be decreased or less active, yet more abundant catalyst materials become feasible. From Fig. 3e, it can be estimated that 21% and 35% of the catalyst loading or activity for the coupled and coupled/insulated case, respectively, could be saved in our test device to achieve the same operation current as in the decoupled configuration. Therefore, thermal coupling also increases the efficiency with respect to the use of catalysts in the device. Note that these numbers depend on the ohmic cell resistance, device configuration, the V_{OC}, and its temperature coefficient as discussed above. Finally, the reduced overpotentials from catalysis and ion transport offer the opportunity to use emerging solar cell material configurations such as III–V/Si tandem configurations, where the challenges of internal interfaces reduce the effective photovoltage.[20] These considerations are highly relevant for the design and commercialisation of highly efficient thermally coupled solar water splitting, which could use III–V/Si[21] or Perovskite/Si[33] tandem cells in a wired design or with the absorber fully immersed in the electrolyte.

Some scientific and engineering challenges remain. For example, overall efficiency would benefit from a device operating at high pressures to eliminate the need for hydrogen compressors. Gaseous products need to be safely separated. The device needs to be demonstrably stable for years, not hours. Nevertheless, we lay the foundation for a thermally tightly coupled water-splitting device that can produce hydrogen under extreme climatic conditions with a maximum degree of autonomy. Our simple concept of insulating photoelectrochemical reactors with low-cost materials can boost the efficiency – both in terms of production rate and catalyst loading – of devices suffering from ohmic or catalysis losses at low temperatures. We clearly demonstrate that the approach of highly integrated solar water splitting, where the absorber is immersed in the electrolyte,[10] can benefit efficiency, though it is technologically challenging. Here, heat transport from absorber to the catalysts is more efficient as the catalyst on the illuminated side is in direct contact with the absorber, while the complementary catalyst can also be in direct contact. The electrolyte is efficiently coupled by convective heat transfer within the PEC cell. Equilibrium temperatures are expected to be higher, as the electrolyte layer on the front reduces the emissivity of the device in the infrared. This would effect efficiencies in a similar manner as device insulation. A hybrid approach is the one used in this work, where the solar cells are not immersed, but thermally coupled, providing technological maturity at the expense of thermal coupling efficiency. Our work offers a pathway for transition to a fossil-fuel-free energy supply in high-latitude and high-altitude areas, and also opens opportunities for decentralised hydrogen production in world regions with less extreme, but still cold outdoor temperatures. This can become a considerable contribution towards the decarbonisation of the energy sector at the global scale.

Open Access Article. Published on 01 Julie 2021. Downloaded on 2026-05-13 5:16:18 vm..
This article is licensed under a Creative Commons Attribution 3.0 Unported Licence.

Author contributions

The project was developed by MM and KR, the experimental design by MK and MM. Code for the photoelectrochemical model was implemented by MK and MM, the experiments conducted by MK, the climate data analysis done by KR. The authors jointly wrote the manuscript.

Conflicts of interest

Helmholtz-Zentrum Berlin, Universität Ulm, and Ruprecht-Karls-Universität Heidelberg have filed a patent application for the concept of insulating electrochemical compartments in thermally coupled water splitting as described above.

Acknowledgements

We thank Fatwa F. Abdi, James Barry, Jesko Fink, Klaus Habicht, Karsten Harbauer, Christian Höhn, Danny Kojda, Konstantin Quoll, and Klaus Schwarzburg for technical support and helpful discussions as well as the HZB's HEMF facility for the infrastructure. Climate data analyses were based on modified Copernicus Climate Change Service information [2021]. Neither the European Commission nor ECMWF is responsible for any use that may be made of this modified Copernicus information. The work was funded by a Volkswagen Foundation Experiment! grant. K. R. and M. M. furthermore acknowledge funding from the German Research Foundation, Projects No. 395588486 and 434023472.

References

1 C. Le Quéré, R. M. Andrew, P. Friedlingstein, S. Sitch, J. Pongratz, A. C. Manning, J. I. Korsbakken, G. P. Peters, J. G. Canadell, R. B. Jackson, T. A. Boden, P. P. Tans, O. D. Andrews, V. K. Arora, D. C. E. Bakker, L. Barbero, M. Becker, R. A. Betts, L. Bopp, F. Chevallier, L. P. Chini, P. Ciais, C. E. Cosca, J. Cross, K. Currie, T. Gasser, I. Harris, J. Hauck, V. Haverd, R. A. Houghton, C. W. Hunt, G. Hurtt, T. Ilyina, A. K. Jain, E. Kato, M. Kautz, R. F. Keeling, K. Klein Goldewijk, A. Körtzinger, P. Landschützer, N. Lefèvre, A. Lenton, S. Lienert, I. Lima, D. Lombardozzi, N. Metzl, F. Millero, P. M. S. Monteiro, D. R. Munro, J. E. M. S. Nabel, S. Nakaoka, Y. Nojiri, X. A. Padin, A. Peregon, B. Pfeil, D. Pierrot, B. Poulter, G. Rehder, J. Reimer, C. Rödenbeck, J. Schwinger, R. Séférian, I. Skjelvan, B. D. Stocker, H. Tian, B. Tilbrook, F. N. Tubiello, I. T. van der Laan-Luijkx, G. R. van der Werf, S. van Heuven, N. Viovy, N. Vuichard, A. P. Walker, A. J. Watson, A. J. Wiltshire, S. Zaehle and D. Zhu, *Earth System Science Data*, 2018, **10**, 405–448.
2 J. A. Turner, *Science*, 2004, **305**, 972–974.
3 M. M. May, H.-J. Lewerenz, D. Lackner, F. Dimroth and T. Hannappel, *Nat. Commun.*, 2015, **6**, 8286.
4 A. Kleidon, L. Miller and F. Gans, in *Physical Limits of Solar Energy Conversion in the Earth System*, ed. H. Tüysüz and C. K. Chan, Springer International Publishing, Cham, 2016, pp. 1–22.
5 M. D. Cabezas, E. A. Wolfram, J. I. Franco and H. J. Fasoli, *Int. J. Hydrogen Energy*, 2017, **42**, 23455–23463.
6 J. L. Aprea, *Int. J. Hydrogen Energy*, 2012, **37**, 14773–14780.
7 R. van de Krol and B. A. Parkinson, *MRS Energy Sustainability*, 2017, **4**, 13.
8 T. J. Jacobsson, *Energy Environ. Sci.*, 2018, **11**, 1977–1979.
9 S. E. Hosseini and M. A. Wahid, *Int. J. Energy Res.*, 2020, **44**, 4110–4131.
10 M. M. May, H. Döscher and J. Turner, in *Integrated Solar Fuel Generators*, ed. I. D. Sharp, H. A. Atwater and H.-J. Lewerenz, The Royal Society of Chemistry, 2018, ch. 12, pp. 454–499.
11 K. Sivula and R. van de Krol, *Nat. Rev. Mater.*, 2016, **1**, 15010.
12 J. T. Davis, J. Qi, X. Fan, J. C. Bui and D. V. Esposito, *Int. J. Hydrogen Energy*, 2018, **43**, 1224–1238.
13 S. Tembhurne, F. Nandjou and S. Haussener, *Nat. Energy*, 2019, **4**, 399–407.
14 I. Bayrak Pehlivan, U. Malm, P. Neretnieks, A. Glüsen, M. Müller, K. Welter, S. Haas, S. Calnan, A. Canino, R. G. Milazzo, S. M. S. Privitera, S. A. Lombardo, L. Stolt, M. Edoff and T. Edvinsson, *Sustainable Energy Fuels*, 2020, **4**, 6011–6022.
15 H. Hersbach, B. Bell, P. Berrisford and S. Hirahara, *Q. J. R. Meteorol. Soc.*, 2020, **146**, 1999–2049.
16 H. Hersbach, B. Bell, P. Berrisford, G. Biavatti, A. Horányi, J. Muñoz Sabater, J. Nicolas, C. Peubey, R. Radu, I. Rozum, D. Schepers, A. Simmons, C. Soci, D. Dee and J.-N. Thépaut, ERA5 hourly data on single levels from 1979 to present, Copernicus Climate Change Service (C3S) Climate Data Store (CDS), 2018, https://doi.org/10.24381/cds.adbb2d47, Accessed on 28-12-2020.
17 I. Y. Ahmet, Y. Ma, J.-W. Jang, T. Henschel, B. Stannowski, T. Lopes, A. Vilanova, A. Mendes, F. Abdi and R. van de Krol, *Sustainable Energy Fuels*, 2019, **3**, 2366–2379.
18 M. M. May and M. Kölbach, YaSoFo - Yet Another SOlar Fuels Optimizer, 2021, https://doi.org/10.5281/zenodo.1489157, Key reference.
19 C. M. Gable, H. F. Betz and S. H. Maron, *J. Am. Chem. Soc.*, 1950, **72**, 1445–1448.
20 R. Cariou, J. Benick, F. Feldmann, O. Höhn, H. Hauser, P. Beutel, N. Razek, M. Wimplinger, B. Bläsi, D. Lackner, M. Hermle, G. Siefer, S. W. Glunz, A. W. Bett and F. Dimroth, *Nat. Energy*, 2018, **3**, 326–333.
21 C. F. Blanco, S. Cucurachi, F. Dimroth, J. B. Guinée, W. J. G. M. Peijnenburg and M. G. Vijver, *Energy Environ. Sci.*, 2020, **13**, 4280–4290.
22 E. Kemppainen, S. Aschbrenner, F. Bao, A. Luxa, C. Schary, R. Bors, S. Janke, I. Dorbandt, B. Stannowski, R. Schlatmann and S. Calnan, *Sustainable Energy Fuels*, 2020, **4**, 4831–4847.
23 M. Reuß, J. Reul, T. Grube, M. Langemann, S. Calnan, M. Robinius, R. Schlatmann, U. Rau and D. Stolten, *Sustainable Energy Fuels*, 2019, **3**, 801–813.
24 N. Roberts and D. Walker, *Int. J. Therm. Sci.*, 2011, **50**, 648–662.

 This journal is © The Royal Society of Chemistry 2021

Open Access Article. Published on 01 Julie 2021. Downloaded on 2026-05-13 5:16:18 vm..
This article is licensed under a Creative Commons Attribution 3.0 Unported Licence.

25 A. J. E. Rettie, W. D. Chemelewski, D. Emin and C. B. Mullins, *J. Phys. Chem. Lett.*, 2016, **7**, 471–479.
26 L. Zhang, X. Ye, M. Boloor, A. Poletayev, N. A. Melosh and W. C. Chueh, *Energy Environ. Sci.*, 2016, **9**, 2044–2052.
27 T. Tin, B. K. Sovacool, D. Blake, P. Magill, S. E. Naggar, S. Lidstrom, K. Ishizawa and J. Berte, *Renewable Energy*, 2010, **35**, 1715–1723.
28 Y. Dou, G. Zuo, X. Chang and Y. Chen, *Appl. Sci.*, 2019, **9**, 1968.
29 S. Wuttke and G. Seckmeyer, *Theor. Appl. Climatol.*, 2006, **85**, 131–148.
30 E. D. Wachsman and K. T. Lee, *Science*, 2011, **334**, 935–939.
31 M. V. Madsen, H. C. Steen-Larsen, M. Hörhold, J. Box, S. M. Berben, E. Capron, A. K. Faber, A. Hubbard, M. F. Jensen, T. R. Jones, S. Kipfstuhl, I. Koldtoft, H. R. Pillar, B. H. Vaughn, D. Vladimirova and D. Dahl-Jensen, *J. Geophys. Res.: Atmos.*, 2019, **124**, 2932–2945.
32 J. Saint-Just and S. Etemad, in *Compendium of Hydrogen Energy*, ed. F. Barbir, A. Basile and T. N. Veziroglu, Woodhead Publishing, Oxford, 2016, pp. 263–287.
33 A. Al-Ashouri, E. Köhnen, B. Li, A. Magomedov, H. Hempel, P. Caprioglio, J. A. Márquez, A. B. Morales Vilches, E. Kasparavicius, J. A. Smith, N. Phung, D. Menzel, M. Grischek, L. Kegelmann, D. Skroblin, C. Gollwitzer, T. Malinauskas, M. Jošt, G. Matič, B. Rech, R. Schlatmann, M. Topič, L. Korte, A. Abate, B. Stannowski, D. Neher, M. Stolterfoht, T. Unold, V. Getautis and S. Albrecht, *Science*, 2020, **370**, 1300–1309.